Available online at www.sciencedirect.com

ScienceDirect

Mendeleev Commun., 2019, **29**, 486–488

Mendeleev Communications

Size effect in nonstoichiometric titanium monoxide and vanadium carbide nanocrystals measured by positron lifetime spectroscopy

Andrey A. Rempel,*[a,b,c] Albina A. Valeeva,[b,c] Alexey S. Kurlov,[b] Gregor Klinser[d] and Wolfgang Sprengel[d]

[a] *Institute of Metallurgy, Ural Branch of the Russian Academy of Sciences, 620016 Ekaterinburg, Russian Federation. Fax: +7 343 267 9186; e-mail: rempel.imet@mail.ru*

[b] *Institute of Solid State Chemistry, Ural Branch of the Russian Academy of Sciences, 620990 Ekaterinburg, Russian Federation. Fax: +7 343 374 4495*

[c] *SEC 'Nanomaterials and Nanotechnologies', Ural Federal University, 620002 Ekaterinburg, Russian Federation*

[d] *Institute of Materials Physics, Graz University of Technology, A-8010 Graz, Austria*

DOI: 10.1016/j.mencom.2019.09.002

A size effect in nonstoichiometric titanium monoxide TiO_y and vanadium carbide VC_y nanocrystals containing high concentrations of structural vacancies was detected by electron-positron annihilation. The effect consists of a considerable increase in the positron lifetime with the specific surface area. An analysis of the intensity of a long lifetime surface component in the positron annihilation spectra and the average positron lifetime for different nonstoichiometric compounds indicated a universal character of the observed size effect.

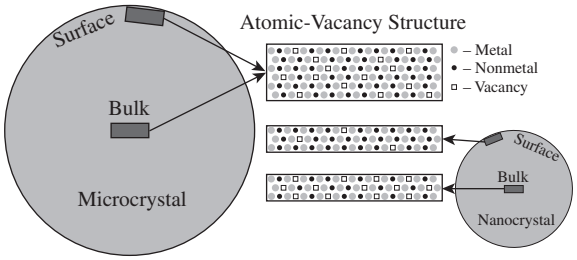

Unlike microcrystals, the nanocrystals of transition metal compounds possess unique properties due to their developed surface area.[1–6] By varying the size, shape, stoichiometry and vacancy ordering of the nanocrystals, it is possible to design nanomaterials with diverse property combinations.[7–12]

At present, non-stoichiometry in nanocrystals is one of the most topical research areas, since owing to non-stoichiometry one can create materials with desired properties by changing the concentration of structural vacancies and by tuning their arrangement in the crystal volume. From the fundamental point of view, it is still an open question how the nanocrystal size affects the ratio of different chemical elements, *i.e.*, their stoichiometry.

In this work, the electron-position annihilation method was used to study the atomic-vacancy structure of titanium monoxide and vanadium carbide nanocrystals, which contain a high concentration of structural vacancies and have a large specific surface. The purpose of this study was to detect a nanocrystal size effect on their specific surface upon advancing from a microcrystal to a nanocrystal.

The microcrystals of titanium monoxide TiO_y with an average particle size of ~25 μm and cubic basic *B*1 structure were synthesized from a mixture of titanium and titanium dioxidemicropowders at 10^{-3} Pa and 1770 K as described in detail elsewhere.[13] The microcrystals of vanadium carbide $VC_{0.875}$ were produced by a high-temperature carbothermal reduction of V_2O_5 micropowder in the presence of amorphous carbon black with the subsequent long-term aging at ambient temperature. The aged vanadium carbide powder contained 18.5 ± 0.1 wt% carbon; thus, the composition $VC_{0.875}$ corresponds to the upper boundary of the homogeneity region of the cubic phase with *B*1 basic structure.[14]

The nanostructuring of the nonstoichiometric titanium monoxide[13,15] and vanadium carbide microcrystals[14] was carried out by high-energy milling in a Retsch PM 200 planetary ball mill (ball-to-powder weight ratio, 10 : 1; milling liquid, isopropanol; milling ball material, ZrO_2 stabilized with Y_2O_3). The following milling mode was used to produce titanium monoxide nanocrystals: total milling duration of 8 h, reversal of the rotation direction every 15 min, rotation direction change in an interval of 5 s, rotation rate of the backing plate of milling cups of 500 rpm. Upon milling, the powders were dried in air at 60 °C. A milling set (balls and cup walls) of cobalt-doped tungsten carbide WC–6 wt% Co was used for the milling of vanadium carbide. Vanadium carbide nanocrystallites were prepared at a total milling duration of 15 h; the rotation rate of the backing plate of milling cups was 500 rpm. After milling, the powders were dried at a residual pressure of 10^4 Pa and a temperature of 85 °C in a Binder VDL 23 vacuum dryer.

The XRD analysis was performed on a Shimadzu XRD-7000 diffractometer in $CuK\alpha_{1,2}$ radiation. The XRD patterns were recorded in the Bragg–Brentano geometry in a stepwise scanning mode with $\Delta(2\theta) = 0.02°$ in a 2θ range of 10–140°. Microcrystalline silicon powder with the cubic lattice constant a = 543.07 pm was used as an external standard. The full-profile analysis of the XRD patterns was carried out using the Powder Cell 2.4 program. The ICDD PDF2 powder diffraction database (2009) was used for phase identification. The diffractometer resolution function was determined using a standard LaB_6 powder (NIST Standard Reference Powder 660a) with a cubic lattice constant of 415.69 pm and a particle size of ~10 μm. The diffractometer resolution function had the parameters u = 0.0058, v = –0.0046 and w = 0.0101.

Microdeformations appeared in the nanoparticles owing to nanostructuring along with a particle size reduction. The size and deformation contributions to the reflection broadening were determined by the Williamson–Hall method.[16] The average vanadium

Table 1 Experimental and theoretical positron lifetimes in the delocalized state, τ_{free}, in vacancies in the metal (M) sublattice, τ_M, and in the nonmetal (X) sublattice, τ_X.

MX_y compound	State	Structure	Positron lifetime τ/ps			Reference
			delocalized state τ_{free}	metal vacancy τ_M	nonmetal vacancy τ_X	
$TiO_{0.74}$–$TiO_{1.26}$	microcrystal	*B*1	140 ± 10	184–210	170 ± 10	[18–20]
$TiO_{1.00}$	nanocrystal	*B*1	–	τ_1 = 205, I_1 = 62% τ_2 = 349, I_2 = 38%	–	This work
m-ZrO_2	microcrystal	$P2_1/c$	174 ± 10	–	–	[21]
ZrO_2–Y_2O_3	nanocrystal	tetragonal, YSZ	170 ± 5	τ_1 = 337 ± 20, I = 5.7%		[21]
$VC_{0.87}$	microcrystal	*B*1		172 ± 1 (after irradiation)	157 ± 2	[22]
			98[a]	147[a]	121[a]	[23]
					τ_1 = 164, I_1 = 75% τ_2 = 339, I_2 = 25%	This work
$VC_{0.87}$	nanocrystal	$P4_332$	–	–	τ_1 = 152, I_1 = 40% τ_2 = 314, I_2 =60%	This work
WC	microcrystal	hexagonal	124 ± 10	175 ± 20	136 ± 3	[24]
			95[a]	161[a]	116[a]	[25]

[a] Calculated values.

carbide nanocrystal size after 15 h of milling was about 20 ± 10 nm, as determined by the extrapolation of the reduced broadening of $\beta^*(2\theta)$ reflections from the length of the scattering vector $s = 2\sin\theta/\lambda$ to $s = 0$. The value of ε for microdeformations was 0.69 ± 0.05%. After milling for 8 h, the minimal nanoparticle sizes for the ordered and disordered titanium monoxide were 20 ± 10 and 40 ± 10 nm, and the microdeformation values were 0.3 ± 0.02 and 0.6 ± 0.04%, respectively.

The positron lifetime spectra of TiO_y and VC_y micro- and nanocrystal samples were measured using a fast-fast coincidence spectrometer with a time resolution of 230 ps (FWHM) and with a general number of coincident counts of more than 10^6 for each spectrum. As a positron source, ^{22}NaCl with an activity between 1 and 2 MBq was used. The source was placed between two identical sample plates. The spectra were numerically processed with an accuracy of 1 ps by multicomponent analysis with the use of the PALSfit program (Ver. 2.80).[17]

Earlier,[18–20] a single component was found in the positron lifetime spectrum for microcrystalline titanium monoxide. The

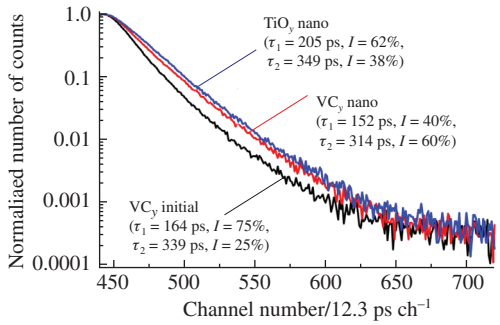

Figure 1 Positron lifetime spectra of TiO_y and VC_y nanocrystals in comparison with a spectrum of VC_y microcrystals.

positron lifetime for both the disordered and ordered titanium monoxide increased from 184 to 210 ps as the oxygen content increased from $TiO_{0.74}$ to $TiO_{1.26}$. According to the analysis of the core electron distribution energy, the local environment of the positron annihilation place is represented by oxygen atoms, suggesting that positrons are trapped exclusively by titanium vacancies.

The positron lifetime spectra were analyzed using fits with several components. The spectra of titanium monoxide nanocrystals were the sums of two short and long components. The short component of 205 ps (I_1 = 62%) corresponds to the localized trap state of a titanium vacancy (Table 1). The other longer component of 349 ps of smaller intensity I_2 = 38% corresponds to the localized state of positron trapping at grain boundaries. Note that the average nanocrystal size in titanium monoxide ranged from 20 to 40 nm, which is shorter than the average diffusion length of a thermalized positron. Consequently, the probability of positron annihilation on the surface and interfaces of particles is very high. It can be assumed that the contribution from the milling balls (ZrO_2–Y_2O_3, 5 wt%) little affects the lifetime since the positron lifetime of tetragonal YSZ (see Table 1) is 337 ± 20 ps,[21] which is very close to the second component in titanium monoxide.

Previously, a single positron lifetime component of 157 ± 2 ps was measured in microcrystalline vanadium carbide VC_y,[22] which was ascribed to positron trapping at a carbon vacancy. The calculated positron lifetimes for bulk and in different vacancies[23] were between 98 and 147 ps (see Table 1). Additionally, the positron lifetime was found to increase from 157 ± 2 to 172 ± 1 ps after the electron bombardment of VC_y. This large difference is explained by changes in the sublattice where positron trapping occurs; before electron bombardment, it was located at a carbon vacancy, while it was at a metal vacancy after bombardment.

The positron lifetime spectrum of VC_y nanocrystals exhibited two components: a component of 152 ps (I_1 = 40%) corresponds to positron annihilation at a carbon vacancy, and the other longer component of 314 ps (I_2 = 60%) corresponds to positron annihilation on the nanocrystal surface. The contribution from the milling balls (cobalt-doped tungsten carbide) slightly affects the lifetime since the positron lifetime of hexagonal WC (see Table 1) is 136 ± 3 ps,[24] which is close to the fist component in VC_y nanocrystals. Note that the positron lifetime spectra of the initial vanadium carbide powders also are the sums of a short and intense component (164 ps, I_1 = 75%) and a longer and less intense component (339 ps, I_2 = 25%) (Figure 1). This means that the initial VC_y already had a developed surface before milling. Upon fragmentation, the surface contribution increased from 25 to 60%.

In addition, pycnometer density measurements, the specific surface areas of the nanopowders, and electron-microscopic and XRD data allowed us to relate the positron lifetime to the specific surface area of the initial TiO_y and VC_y crystals and the nanocrystals (Table 2). We found that the positron lifetime of nanocrystals is directly proportional to the specific surface area (Figure 2), and the experimental data were described by the function: $\tau_{mean} = \tau_{crystal} + k\,S_{sp}$, where S_{sp} is the specific surface area of the nanocrystals, and k is an empirical constant.

An increase in the surface area upon nanostructuring affects the specific lattice sites of positron trapping in nanocrystals. The

Table 2 Pycnometer density and specific surface area of nonstoichiometric compounds in micro- and nanostates.

Compound	ρ/g cm^{-3}	S_{sp}/m^2 g^{-1}	d_{mean}/nm	τ_{mean}/ps
TiO_y initial	4.931 ± 0.002	2.29 ± 0.06	530	200
TiO_y nano	4.551 ± 0.004	43.95 ± 0.5	30	260
VC_y initial	5.125 ± 0.003	2.45 ± 0.03	480	208
VC_y nano	4.956 ± 0.003	33.3 ± 0.4	30	250

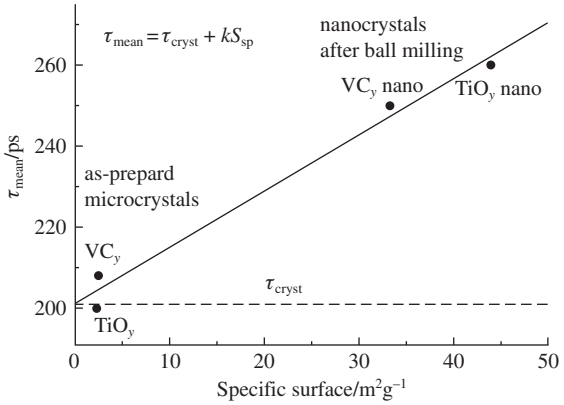

Figure 2 Dependence of the positron lifetime on the specific surface area of as-prepared microcrystals and nanocrystals after the ball milling of TiO_y and VC_y.

positron lifetimes detected in TiO_y (205 and 349 ps) can be related to positron annihilation in titanium vacancy in the nanocrystal volume and at a trap site on the crystal surface, respectively. The contribution of the specific surface to the positron lifetime is 38%. An increase in the surface contribution for VC_y nanocrystals from 25 to 60 % leads to an enhancement of the positron lifetime from 152 to 339 ps.

Thus, we found that the positron lifetime in nanocrystals is directly proportional to the specific surface area. The detected size effect should be considered in an interpretation of the structure and properties of the nanocrystals of nonstoichiometric compounds. This effect can be used for designing functional materials with unusual physical properties.

The work was carried out in accordance with the Russian state assignment for the Institute of Metallurgy of the Ural Branch of the Russian Academy of Sciences and the Institute of Solid State Chemistry of the Ural Branch of the Russian Academy of Sciences. Additionally this work was financially supported by the end of 2018 by the Russian Science Foundation (grant no. 14-23-00025).

References

1 D. Wrana, C. Rodenbücher, B. R. Jany, O. Kryshtal, G. Cempura, A. Kruk, P. Indyka, K. Szot and F. Krok, *Nanoscale*, 2019, **11**, 89.
2 J. Xu, D. Wang, H. Yao, K. Bu, J. Pan, J. He, F. Xu, Z. Hong, X. Chen and F. Huang, *Adv. Mater.*, 2018, **30**, 1706240.
3 X. Chen and S. S. Mao, *Chem. Rev.*, 2007, **107**, 2891.
4 P. Simon, B. Pignon, B. Miao, S. Coste-Leconte, Y. Leconte, S. Marguet, P. Jegou, B. Bouchet-Fabre, C. Reynaud and N. Herlin-Boime, *Chem. Mater.*, 2010, **22**, 3704.
5 B. M. Pabón, J. I. Beltrán, G. Sánchez-Santolino, I. Palacio, J. López-Sánchez, J. Rubio-Zuazo, J. M. Rojo, P. Ferrer, A. Mascaraque, M. C. Muñoz, M. Varela, G. R. Castro and O. Rodriguez de la Fuente, *Nat. Commun.*, 2015, **6**, 6147.
6 A. S. Bolokang, D. E. Motaung, C. J. Arendse and T. F. G. Muller, *Mater. Charact.*, 2015, **100**, 41.
7 T.-T.-N. Nguyen and J.-L. He, *Adv. Powder Technol.*, 2016, **27**, 1868.
8 H.-E. Schaefer, *Nanoscience: The Science of the Small in Physics, Engineering, Chemistry, Biology and Medicine*, Springer-Verlag, Berlin, Heidelberg, 2010.
9 J. Xu, Z. Tian, G. Yin, T. Lin and F. Huang, *Dalton Trans.*, 2017, **46**, 1047.
10 V. Jandová, Z. Bastl, J. Šubrt and J. Pola, *J. Anal. Appl. Pyrol.*, 2011, **92**, 287.
11 J. Blazevska-Gilev, V. Jandová, J. Kupčik, Z. Bastl, J. Šubrt, P. Bezdička and J. Pola, *J. Solid State Chem.*, 2013, **197**, 337.
12 A. A. Valeeva, E. A. Kozlova, A. S. Vokhmintsev, R. V. Kamalov, I. B. Dorosheva, A. A. Saraev, I. A. Weinstein and A. A. Rempel, *Sci. Rep.*, 2018, **8**, 9607.
13 A. A. Valeeva, S. Z. Nazarova and A. A. Rempel, *Phys. Solid State*, 2016, **58**, 771 (*Fiz. Tverd. Tela*, 2016, **58**, 747).
14 A. S. Kurlov, A. I. Gusev and A. A. Rempel, *Mendeleev Commun.*, 2014, **24**, 338.
15 S. V. Rempel, A. A. Valeeva, E. A. Bogdanova, H. Schroettner, N. A. Sabirzyanov and A. A. Rempel, *Mendeleev Commun.*, 2016, **26**, 543.
16 W. H. Hall and G. K. Williamson, *Proc. Phys. Soc., Sect. B*, 1951, **64**, 937.
17 P. Kirkegaard, M. Eldrup, O. E. Mogensen and N. J. Pedersen, *Comput. Phys. Commun.*, 1981, **23**, 307.
18 A. A. Valeeva, A. A. Rempel, W. Sprengel and H.-E. Schaefer, *Phys. Rev. B*, 2007, **75**, 094107.
19 A. A. Valeeva, A. A. Rempel, W. Sprengel and H.-E. Schaefer, *Phys. Chem. Chem. Phys.*, 2003, **5**, 2304.
20 A. A. Valeeva, A. A. Rempel, W. Sprengel and H.-E. Schaefer, *Phys. Solid State*, 2009, **51**, 924 (*Fiz. Tverd. Tela*, 2009, **51**, 876).
21 H.-E. Schaefer and M. Forster, *Mater. Sci. Eng., A*, 1989, **109**, 161.
22 A. A. Rempel, L. V. Zueva, V. N. Lipatnikov and H.-E. Schaefer, *Phys. Status Solidi A*, 1998, **169**, R9.
23 M. J. Puska, M. Šob, G. Brauer and T. Korhonen, *Phys. Rev. B*, 1994, **49**, 10947.
24 A. A. Rempel, R. Würschum and H.-E. Schaefer. *Phys. Rev. B*, 2000, **61**, 5945.
25 M. J. Puska, M. Sob, G. Brauer and T. Korhonen, *J. Phys. IV*, 1995, **5**, 135.

Received: 25th February 2019; Com. 19/5841